One month in the life of a neuron: longitudinal single-unit electrophysiology in the monkey visual system

David B. T. McMahon, Igor V. Bondar, Olusoji A. T. Afuwape, David C. Ide and David A. Leopold

J Neurophysiol 112:1748-1762, 2014. First published 25 June 2014; doi:10.1152/jn.00052.2014

You might find this additional info useful...

Supplemental material for this article can be found at:
/content/suppl/2014/08/07/jn.00052.2014.DC1.html

This article cites 65 articles, 29 of which can be accessed free at:
/content/112/7/1748.full.html#ref-list-1

Updated information and services including high resolution figures, can be found at:
/content/112/7/1748.full.html

Additional material and information about ***Journal of Neurophysiology*** can be found at:
http://www.the-aps.org/publications/jn

This information is current as of November 10, 2014.

Journal of Neurophysiology publishes original articles on the function of the nervous system. It is published 12 times a year (monthly) by the American Physiological Society, 9650 Rockville Pike, Bethesda MD 20814-3991. Copyright © 2014 by the American Physiological Society. ISSN: 0022-3077, ESSN: 1522-1598. Visit our website at http://www.the-aps.org/.

Downloaded from on November 10, 2014

J Neurophysiol 112: 1748–1762, 2014.
First published June 25, 2014; doi:10.1152/jn.00052.2014.

One month in the life of a neuron: longitudinal single-unit electrophysiology in the monkey visual system

David B. T. McMahon,[1] Igor V. Bondar,[2] Olusoji A. T. Afuwape,[1] David C. Ide,[3] and David A. Leopold[1,4]

[1]*Section on Cognitive Neurophysiology and Imaging, National Institute of Mental Health, National Institutes of Health, Bethesda, Maryland;* [2]*Institute of Higher Nervous Activity and Neurophysiology, Moscow, Russia;* [3]*Section on Instrumentation, National Institute of Mental Health, National Institutes of Health, Bethesda, Maryland; and* [4]*Neurophysiology Imaging Facility, National Institute of Mental Health, National Eye Institute, and National Institute of Neurological Disorders and Stroke, National Institutes of Health, Bethesda, Maryland*

Submitted 17 January 2014; accepted in final form 23 June 2014

McMahon DB, Bondar IV, Afuwape OA, Ide DC, Leopold DA. One month in the life of a neuron: longitudinal single-unit electrophysiology in the monkey visual system. *J Neurophysiol* 112: 1748–1762, 2014. First published June 25, 2014; doi:10.1152/jn.00052.2014.—Conventional recording methods generally preclude following the activity of the same neurons in awake animals across days. This limits our ability to systematically investigate the principles of neuronal specialization, or to study phenomena that evolve over multiple days such as experience-dependent plasticity. To redress this shortcoming, we developed a drivable, chronically implanted microwire recording preparation that allowed us to follow visual responses in inferotemporal (IT) cortex in awake behaving monkeys across multiple days, and in many cases across months. The microwire bundle and other implanted components were MRI compatible and thus permitted in the same animals both functional imaging and long-term recording from multiple neurons in deep structures within a region the approximate size of one voxel (<1 mm). The distinct patterns of stimulus selectivity observed in IT neurons, together with stable features in spike waveforms and interspike interval distributions, allowed us to track individual neurons across weeks and sometimes months. The long-term consistency of visual responses shown here permits large-scale mappings of neuronal properties using massive image libraries presented over the course of days. We demonstrate this possibility by screening the visual responses of single neurons to a set of 10,000 stimuli.

fMRI; macaque; object recognition; physiology; vision

NEURONS THROUGHOUT THE BRAIN show specialized patterns of activity in relation to specific sensory, motor, or cognitive events. Understanding the nature of this specialization lies at the heart of investigations into the functional organization of brain systems. Since the final output of the nervous system is driven by the coordinated action of neuronal circuits, the advantage of monitoring populations of neurons simultaneously is widely recognized (Alivisatos et al. 2012; Churchland et al. 2007; Cohen and Maunsell 2009; Nicolelis et al. 2003). Complementary to the approach of studying neuronal function by assessing activity patterns across cells, key insights may also be gained by investigating how neuronal activity changes across time. The properties of single neurons are by necessity shaped by plasticity during early development and by experience with the environment later in life. Accordingly, in seeking to understand the significance of neuronal specialization, we need to ask how neurons acquire their individual response properties and how they are affected by experience.

At present, physiological studies assessing the response profile of individual cells are usually limited to a single recording session lasting a few hours. Because many real-world instances of learning and plasticity take place on much longer timescales of days or weeks, this technical constraint imposes a fundamental limit on our ability to assess how experience drives neuronal changes. In studies assessing the acquisition of motor skills (Karni et al. 1998; Matsuzaka et al. 2007; Sanes and Donoghue 2000) or perceptual expertise (Ghose et al. 2002; Karni and Sagi 1993; Schoups et al. 2001), improvements in behavioral performance commonly emerge after repeated training sessions spread out over multiple days. Plasticity likewise alters the properties of neuronal circuits during the first few weeks after birth (Espinosa and Stryker 2012) or in transient periods after injury (Merzenich et al. 1984; Recanzone et al. 1992). Since conventional physiological recording methods provide only a snapshot of neuronal response properties at a single point in time, our understanding of plastic changes expressed over prolonged periods necessarily relies on sampling separate populations of neurons before and after learning (De Baene et al. 2008; Freedman and Assad 2006) or on comparisons between neuronal activity in trained vs. untrained conditions (Baker et al. 2002; Sigala and Logothetis 2002). The ability to routinely follow the activity of single neurons on the timescales relevant to long-term learning and plasticity would make it possible to investigate neural mechanisms of learning, development, and the recovery of brain function at a new level of precision and clarity.

Longitudinal tracking of single units is also of interest in contexts where plasticity is not likely to be a factor, and stable neuronal response properties might therefore be expected. In high-level sensory areas, neurons commonly show complex patterns of stimulus selectivity that cannot be readily accounted for by a set of simple feature parameters (DiCarlo et al. 2012; Gross et al. 1972; Kourtzi and Connor 2011). Similarly, neurons in primary motor cortex are sensitive to a broad range of movement parameters over and above their tuning for direction of motion (Scott 2008; Sergio et al. 2005). Thus neuronal activity evidently reflects specialization within a high-dimensional feature space in which the relevant parameters are largely unknown. For this reason, many of the earliest discov-

Address for reprint requests and other correspondence: D. B. T. McMahon, Laboratory of Sensorimotor Research, National Eye Inst., Bldg. 49, Rm. 2A5049, 49 Convent Dr., Bethesda, MD 20982-4435 (e-mail: mcmahond@mail.nih.gov).

Downloaded from on November 10, 2014

eries of neuronal specialization were not at all systematic but literally resulted from trial and error (Gross et al. 1972; Hubel and Wiesel 1998). An automated version of this strategy that has emerged in recent years for dealing with the complexity of neuronal representations is to record activity driven by large stimulus sets and then search for systematic trends in a largely data-driven manner (David et al. 2006; Kiani et al. 2007). Sophisticated genetic algorithms can greatly enhance the efficiency of the exhaustive searches of neuronal feature spaces that such methods entail (Hung et al. 2012; Yamane et al. 2008). Nonetheless, their success ultimately depends on the number of trials it is possible to obtain for a single neuron. Extending the range of a single experiment to encompass multiple days could therefore shed new light on the principles underlying neuronal specialization.

Several examples of recordings across sessions have been demonstrated (Bondar et al. 2009; Fraser and Schwartz 2012; Jackson and Fetz 2007; Mankin et al. 2012; Richardson et al. 2012; Tolias et al. 2007), illustrating that it is in principle possible to maintain stable isolations of single cells. Nonetheless, the potential of longitudinal recordings lies in the future and rests on technology that allows for flexible and robust long-term isolations. In this article, we present a straightforward method for isolating and maintaining single neurons in macaque monkeys with a microwire electrode bundle introduced through an adjustable microdrive. The method is compatible with functional magnetic resonance imaging (fMRI), allowing one to connect single-unit selectivity with regional stimulus preferences. We demonstrate the potential of this technique for addressing experimental questions that are beyond the reach of conventional methods that restrict observations of neuronal properties to single-day recording sessions.

MATERIALS AND METHODS

Subjects

Four chronic electrodes were implanted in three rhesus macaques. Lab designations were SI (monkey *m1*, female, 5.0 kg), TO (monkey *m2*, female, 5.6 kg), and RH (monkey *m3*, male, 8.7 kg). Monkey *m2* received bilateral electrode implants; *m1* and *m3* received left and right hemisphere implants, respectively. All procedures were approved by the Animal Care and Use Committee and complied with the regulations of the National Institute of Mental Health (NIMH) and the National Institutes of Health (NIH).

Apparatus

Microwire electrode bundle. Electrodes were constructed from bundles of 32 or 64 microwires (12-μm diameter, NiCrAl or PtIr alloy) insulated with polyimide. The microwires were threaded through a polyimide-wrapped silica shaft (outer diameter 630 μm, inner diameter 500 μm) that was laser cut to 55-mm length (TSP530660, Polymicro Technologies, Phoenix, AZ). The tips of the wires extended 5 mm past the bottom of the silica shaft and were glued in place. A tail of wires ran 60 mm from the top end of the shaft to a block of two or four 16-pin connectors (A70242-001, Omnetics, Minneapolis, MN). The mean impedance prior to implantation was 0.7 MΩ for PtIr wires and 1.5 MΩ for NiCrAl wires measured with a 1,000-Hz alternating current and a Nipod multichannel impedance tester (NeuroNexus Technologies, Ann Arbor, MI). Construction of the microwire bundles followed procedures described previously (Bondar et al. 2009; Porada et al. 2000), at first using in-house production capabilities and later purchased commercially (Microprobes, Gaithersburg, MD).

Guide tube. Electrode shafts were inserted into the brain through a 760-μm-diameter polyimide guide tube lined with PTFE (MicroLumen, Oldsmar, FL). Guide tubes were cut to 45-mm lengths prior to surgery.

Chronic recording chamber and alignment post. Three-dimensional computer models of the chamber and microdrive components are available in the Supplemental Material for this article.[1] The recording chamber was a cylinder of 22.9-mm height machined from a 3/4-in.-diameter Ultem plastic rod (Fig. 1, *A* and *B*). The base of the chamber was textured to increase the surface area of contact with acrylic. A 6.35-mm-diameter hole was drilled through the length of the chamber at an eccentric position relative to the center of the cylinder (center-to-center offset 5.08 mm). The hole fit over a separate cylindrical alignment post (6.23-mm diameter, 9.17-mm height), which when put together formed a well of adjustable depth that could be filled with silicone sealant. The guide tube and electrode shaft passed through a 0.89-mm hole drilled through the center of the alignment post.

Chronic microdrive. The microdrive was constructed from three Ultem disks (15.88-mm diameter, 4.06-mm height) held together by three ceramic or G10 resin rods (3.18-mm diameter, 25.4-mm height) and a PEEK drive screw held captive between the upper and lower Ultem plates (15-mm length, 0.7-mm pitch; Fig. 1, *A* and *B*). The electrode was clamped into the middle drive disk, the position of which moved 700 μm per revolution of the drive screw. The electrode was further stabilized by a second clamp in the lower disk. The height of the drive permitted a total of 7.5-mm travel. This range could be extended further by fastening the lower clamp and adjusting the position of the upper clamp. The foot of each rod extended 2.5 mm past the bottom of the microdrive and mated with three holes drilled in corresponding positions on the top face of the chamber. The drive was fastened to the chamber by means of two 4-40 nylon screws (1/4-in. length). Turning the drive screw caused the whole electrode bundle to move as one unit; it was not possible to advance the microwires individually.

Protective cap. Because all entry points to the brain were entirely sealed in silicone and the connector block was embedded in acrylic outside the chamber (as described below in *Surgical Procedures*), the chamber only needed to be accessed for the purpose of advancing the electrode. At all other times the chamber and microdrive remained covered by a protective cap (18.45-mm inner diameter, 25.5-mm outer diameter, 31.75-mm inner clearance, 34.15-mm outer height).

Surgical Procedures

All procedures were approved by the NIMH Animal Care and Use Committee and complied with the regulations of NIMH and NIH. Four chronic microwire electrodes were implanted in three monkeys. Presurgical planning was based on structural T1-weighted images obtained on a 1.5T General Electric Signa scanner. The recording target and electrode trajectory were selected to position the electrode tips in regions of interest around the superior temporal sulcus (STS). Two of the monkeys further participated in functional scans conducted presurgically on a vertical 4.7-T scanner (Bruker). In these two cases, the monkeys were fitted with MRI-compatible head posts in a previous surgery. In the third monkey the head post and chronic electrode were implanted in a single surgery. When available, results from functional scans were used to target recording sites in areas within the STS with strong selectivity for face stimuli.

On the morning of the surgery the monkey was sedated with ketamine, diazepam, and glycopyrrolate. Vital signs were monitored continuously while anesthesia was maintained under isoflurane. A

[1] Supplemental Material for this article is available online at the Journal website.

Downloaded from on November 10, 2014

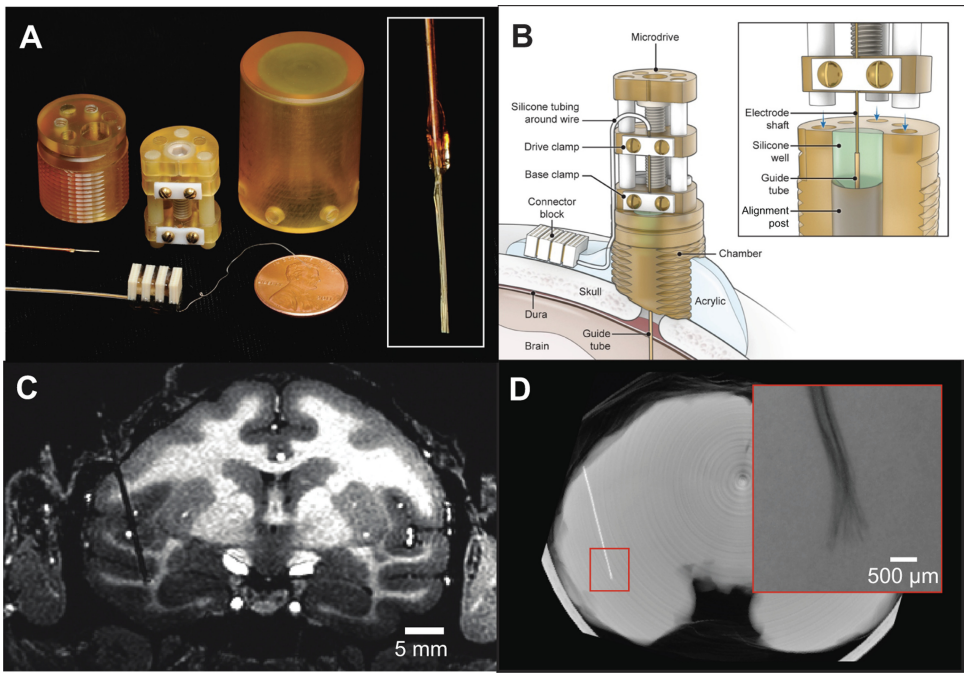

Fig. 1. Chronic recording apparatus and implant. *A*: components used for electrode implantation. The recording chamber, microdrive, and protective cap were machined from biocompatible plastic and contained minimal metal components so as to permit postsurgical functional MRI scanning. Three-dimensional models of the chamber and microdrive are available in the Supplemental Material for this article. *Inset*: close-up photo of wire bundle tip prior to insertion. *B*: electrode and chamber arrangement after implant surgery. The electrode could be periodically advanced postsurgically by turning a screw on the microdrive and otherwise remained covered by the protective cap. The microwire bundle entered the brain through a transdural polyimide guide tube. The junction of the electrode shaft and guide tube was sealed inside a silicone well; thus no routine maintenance was required to prevent infection. *C*: structural MRI showing electrode track and final recording site in the IT cortex of monkey *m1*. *D*: micro-CT reconstruction showing the location of the implanted electrode in the brain in an ex vivo scan. The microwire tips fanned out slightly in the cortex but remained within a 1-mm radius (*inset*, radiograph).

craniotomy hole (~3-mm diameter) was drilled in the skull to allow access to the dura. The guide tube was placed on a 22-gauge spinal needle that was mounted in a stereotaxic micromanipulator (David Kopf Instruments, Tujunga, CA). After the needle tip pierced the dura, the guide tube was lowered into the cortex until the end of the guide tube was 3–4 mm dorsal to the STS, based on the depth determined from the presurgical MRI scan. The outside of the guide tube was then glued in place to the alignment post so that it remained a fixed depth inside the brain. The craniotomy hole was filled with bone wax, and the alignment post was cemented to the surrounding skull with acrylic anchored by ceramic bone screws. After the acrylic hardened, the insertion needle was withdrawn from the guide tube and the chamber was sited on the skull using the degree of freedom afforded by rotation of the eccentric cylindrical well around the alignment post. The bottom of the chamber was shaped to match the contour of the skull with a handheld drill. Once sufficient material was removed from the chamber to achieve a dorsal-ventral positioning that allowed the electrode to reach the deepest intended target inside the brain, the chamber was cemented in place with acrylic. Then the top of the guide tube was cut a level ~2 mm below the top face of the chamber. This ensured that, after the electrode was inserted, the junction between the guide tube and electrode shaft would lie below the surface of the silicone sealant.

The electrode was clamped into the microdrive, and the exposed tips of the wire bundle were threaded into the top of the guide tube with an xyz-micromanipulator (David Kopf Instruments). After the microdrive was fastened to the chamber with nylon screws, the electrode was advanced slowly by turning the drive screw until the electrode tips extended 1 mm past the end of the guide tube, which typically placed them in the white matter dorsal to the STS. The chamber well was then filled with silicone (Kwik-Cast Sealant, World Precision Instruments, Sarasota, FL) to seal the junction between the guide tube and the electrode shaft. The purpose of the silicone seal was to close a possible route to infection inside the brain, while still remaining pliable enough to allow the electrode to advance deeper into the brain while the guide tube remained at a fixed depth. The wire tail of the electrode was then routed through a groove drilled in the side of the chamber, and the connector block was cemented to the acrylic cap outside the chamber. One week after the implant surgery, an MRI scan was conducted in order to localize the position of the electrode and to detect potential signs of brain infection. If warranted by the results of the postsurgical scan (as occurred in 2 cases, *m1* and *m3*), the animals received a course of treatment with gentamicin and Claforan antibiotics and a follow-up scan after 2 wk. Since the craniotomy and guide tube were completely encased in the acrylic, plastic, and silicone components of the implant and chronic chamber, no routine cleaning of the chamber was possible or necessary.

Physiological Recording Procedure

Each day, the setup for electrophysiology recordings involved restraining the head and plugging the amplifier cable into the implanted connector block, a procedure requiring just a few minutes. When repositioning of the electrode was performed between stretches of longitudinal recording, this procedure was carried out in the awake animal while it sat in the recording booth. The protective cap was removed and the z-axis screw was rotated to advance the electrode, typically in 350- to 700-μm steps. The cap was only removed for the purpose of advancing the electrode and remained in place throughout other recording days. Our experience indicated that it was unnecessary to put any protective cover over the connector block. In light of observations from our initial studies indicating that neural isolations tended to appear gradually after positional adjustment, the electrode was never adjusted more frequently than once every 3 days. In general, we only moved the electrode if the yield was unsatisfactory and the recording quality did not continue to improve from day to day. The criteria of assessing recording conditions were subjective and included presence of isolated spikes, visual responsiveness of spikes, and presence of audible visually evoked hash arising from small multiunit activity. Experimental data collection commenced once well-isolated single-unit activity was detected on multiple channels, at least some of which also showed obvious visual responses.

Physiological recordings were carried out in an RF-shielded room. Data were collected with either a Multichannel Acquisition Processor (Plexon, Dallas, TX) with 32-channel capacity or a RS4 Bioamp Processor (Tucker-Davis Technologies, Alachua, FL) with 128-channel capacity. Daily recording sessions began 2–4 wk after the initial surgery. Broadband electrophysiological responses (0.5 Hz–5 kHz) were collected, from which individual spikes were extracted and analyzed (see *Data Analysis*). The ground and reference were connected to one another and to a designated reference wire within the microwire bundle as well as to a gold-plated grounding terminal

Downloaded from on November 10, 2014

adjacent to the dura by a ceramic screw placed ~1 cm from the implant margin.

Task and Stimuli

Visual stimuli consisting of diverse natural and artificial images were presented briefly on a computer monitor as the monkey fixated a small point in the center of the screen. The monitor, either a ViewSonic 18-in. CRT display or a Eizo 17-in. LCD monitor, was placed 91 cm in front of the monkey. The monkey initiated each series of trials of the task by maintaining fixation within a 3° window around a 0.3° white fixation dot. In this article, "one trial" is defined as one visual stimulation cycle consisting of a 300-ms stimulus-on interval followed by a 300-ms stimulus-off interval. The monkey was rewarded with a drop of fruit juice or water for maintaining fixation throughout four trials. The stimuli used in standard longitudinal experiments typically fell within a 6.9° window. Visual stimuli were presented one at a time behind the fixation spot, selected in random order without replacement from a stimulus library consisting of 27, 72, 96, or 144 unique images. Stimuli included sets of human faces, monkey faces and whole bodies, dogs, birds, butterflies, fish, flowers, and complex geometrical patterns as well as colorful images belonging to no particular object category. Typically 32–40 trials per stimulus were collected each day. A separate experiment employed a set of 10,000 stimuli, which included 1,000 images drawn from each of the following 10 categories: human faces, human bodies, monkey faces, monkey bodies, birds, butterflies, plants, man-made objects, scenes, and Fourier descriptor patterns. The human faces were drawn from the FEI face database (Thomaz and Giraldi 2010). The monkey faces and bodies were provided courtesy of Dr. Olga Dal Monte. The Fourier descriptors were generated in MATLAB (MathWorks, Natick, MA). Images from all other stimulus categories were assembled from web searches or iPhone applications. All aspects of the task related to stimulus presentation, eye position monitoring, and reward delivery were controlled by custom software courtesy of Dr. David Sheinberg running on a QNX computer. Visual stimuli were presented by a graphics slave computer running the Psychophysics Toolbox (Brainard 1997) in MATLAB. Eye position was monitored via an infrared camera and converted into analog voltage signals corresponding to x and y coordinates by the software EyeLink (SR Research, Kanata, ON, Canada).

Functional Imaging Procedures

The MR compatibility of the microelectrodes, microdrive, and connector was demonstrated by collecting functional scans postsurgically, which likewise verified that exposure to scanning conditions did not compromise the quality of physiological recordings. Functional scans were collected on a 4.7-T vertical scanner (Bruker BioSpin, Rheinstetten, Germany) using T2*-weighted echo planar image (EPI) acquisition sequences. Voxel resolution was 1.5 mm isotropic, with 40 sagittal slices providing coverage of the entire brain. Higher-resolution (0.5 mm isotropic) anatomical scans were collected with modified driven equilibrium Fourier transform (MDEFT) scans, which were collected in separate sessions and registered to the EPI. Functional imaging was based on detection of monocrystalline iron oxide nanocompound (MION; Leite et al. 2002) signal in *m1* and blood oxygenation level-dependent (BOLD) signal in *m2*.

Functional mapping was achieved through presentation of 24-s blocks consisting of baseline fixation, presentation of faces, and presentation of common objects. Such stimuli are commonly used to stimulate the visual cortex, as well as to identify regions selectively responsive to the individual stimulus categories. During each scan 12 blocks were presented, with testing sessions consisting of 10–12 such scans. The functional data were run through a standard preprocessing sequence, including magnetic field distortion correction using the PLACE algorithm (Xiang and Ye 2007), motion correction implemented in AFNI (Cox 1996), and high-pass filtering with a cutoff of 0.01 Hz. The effects of the electrode bundle and plastic microdrive on detectable fMRI signal were evaluated with custom-written software in MATLAB.

Data Analysis

Spikes from single units were sorted with the Offline Sorter software package (Plexon) by projecting waveforms into principal component space and identifying isolated clusters. Spikes were detected either online (with the Plexon acquisition system) or offline (with the Tucker-Davis acquisition system) by setting a trigger threshold to capture a snippet of the voltage trace filtered between 300 and 5,000 Hz. The trigger threshold was set manually for each channel with the goal of satisfying two simultaneous constraints. The first constraint was to maximize the separation of spike clusters in principal component space, both between simultaneously recorded neurons and between each neuron and the baseline noise. The second constraint was to apply a set of sorting decisions that lead to consistent isolation quality [in terms of cluster separation and shape of interspike interval (ISI) histograms] for the same channel across multiple days. The experimenter sought to satisfy both constraints simultaneously, and adjusted the trigger threshold if necessary to compensate for day-to-day changes in the amplitude or isolation of spikes that were suspected of arising from the same neuron.

Waveforms detected on the same channel on different days were tentatively classified as belonging to the same neuron if the waveform and spiking statistics matched between consecutive days as described previously (Bondar et al. 2009). Assessment of unit identity was further tested by computing a stability index based in the reproducibility of stimulus-selective visual responses.

$$\text{stability index} = \left(\mathbf{r}_{\text{across}} - \mathbf{r}_{\text{shuffle}}\right) / \left(\mathbf{r}_{\text{within}} - \mathbf{r}_{\text{shuffle}}\right)$$

In this analysis, Each $\mathbf{r}$ value is a correlation coefficient for two spike count vectors constructed by concatenating a series of averaged firing rates within a fixed window starting 80 ms and ending 450 ms after stimulus onset. Since we found that this poststimulus period adequately captured the visual response in the large majority of cases, the same time window was used to compute the average responses of all neurons. The two vectors for $\mathbf{r}_{\text{within}}$ were obtained by dividing responses collected on one day into odd and even trials. The correlation for $\mathbf{r}_{\text{across}}$ was computed for the same number of odd and even trials recorded on consecutive days, and $\mathbf{r}_{\text{shuffle}}$ was computed after splitting the within-day data into two halves and then shuffling the stimulus identities for one of the two response vectors. Longevity of stable recordings was assessed by comparing the percent change across days

$$\left(\mathbf{r}_{\text{within}} - \mathbf{r}_{\text{across}}\right) / \mathbf{r}_{\text{within}}$$

to the percent change obtained in the stimulus-shuffled control condition

$$\left(\mathbf{r}_{\text{within}} - \mathbf{r}_{\text{shuffle}}\right) / \mathbf{r}_{\text{within}}$$

Statistical analysis was carried out for specific experiments as described in the text with custom software written in MATLAB.

RESULTS

Implantation of Chronic Microwire Electrodes

With the goal of routinely monitoring the activity of single neurons in the brain on a longitudinal basis, we developed a drivable chronic microwire recording technique that was compatible with MRI. The recording preparation comprised a bundle of microwires (32 or 64) that were fixed inside a polyimide-wrapped silica shaft, a chronically implanted re-

Downloaded from on November 10, 2014

cording chamber, and a permanently mounted microdrive (Fig. 1*A*). In an initial surgical procedure, the microwires were lowered into the brain inside a silica shaft that passed through the plastic recording chamber implanted on top of the skull (Fig. 1*B*). The electrode shaft entered the brain through a Teflon-lined polyimide guide tube that was sealed within a silicone well inside the chamber (Fig. 1*B*, *inset*). The electrode shaft was periodically advanced postsurgically by turning the microdrive screw and was otherwise covered by a protective cap. The advancing procedure drove the microwire bundle as a single bulk unit, as it was not possible to move individual microwires independently. The electrode was accessed electrically by plugging into a nickel-free connector block cemented outside the chamber. The entire assembly was free of ferromagnetic materials and contained minimal metallic components so as to permit fMRI in the same animals.

Four microwire electrodes were implanted in the inferotemporal (IT) cortex of three adult rhesus macaque monkeys (*m1*: left hemisphere, *m2*: right hemisphere, *m3*: bilateral electrode implants). All recording sites fell within the STS (*m1*: fundus, *m2*: upper bank, *m3*: lower bank), targeting locations 16 mm (*m1* and *m2*) or 19 mm (*m3*) anterior to the intra-aural canal. During the implantation surgery, the tips of the microwire bundles were lowered into the white matter above the upper bank of the STS (Fig. 1*C*). After a 2-wk recovery period, the electrode was advanced every few days in 300- to 700-μm steps into the gray matter around the sulcus until visually responsive cells were encountered. Evidence from an ex vivo micro-CT scan of the brain from *m1* revealed that the microwire tips fanned out slightly but remained within a 1-mm diameter of brain tissue (Fig. 1*D*). The recordings obtained thus sampled neuronal activity that would typically fall within a single MRI voxel. Monkeys *m1* and *m2* were used in longitudinal experiments in which the same visual stimuli were presented repeatedly over multiple days. Data collection proceeded for 762 days after surgery in *m1* and is ongoing in *m2* (currently beyond 2 yr postsurgery). In *m3* the electrode was removed at 146 days after surgery following the emergence of stickiness within the guide tube that prevented the electrode from being advanced further. While data collection was possible in *m3*, the monkey was used in other experiments involving movie stimuli that are not included here. In total, the cumulative postsurgical implant history in all three monkeys exceeded three and a half years. Significantly, there were no cases of clinical symptoms related to the implanted electrodes during this time.

Compatibility of Longitudinal Recording with Functional Imaging

To assess the compatibility of the electrodes with MRI, we collected functional scans while the monkeys fixated during alternating blocks of visual stimulation and blank intervals. The contrast between visual stimulation vs. blank epochs yielded robust activation throughout the ventral visual pathway, from V1 in the occipital lobe down to anterior IT in the ventral temporal lobe (Fig. 2, *A–C*). Thus, at the global level of functional brain mapping, the susceptibility artifact due to the microwires, connector block, and chamber assembly interfered minimally with the measurement of hemodynamic signal. In the voxels containing the electrode, the magnetic susceptibility of the metal wires precluded detection of functional signal. However, visual responses were measurable in the cube of voxels immediately surrounding the electrode tip (Fig. 2*D*). As noted below, obtaining functional scans in monkeys with

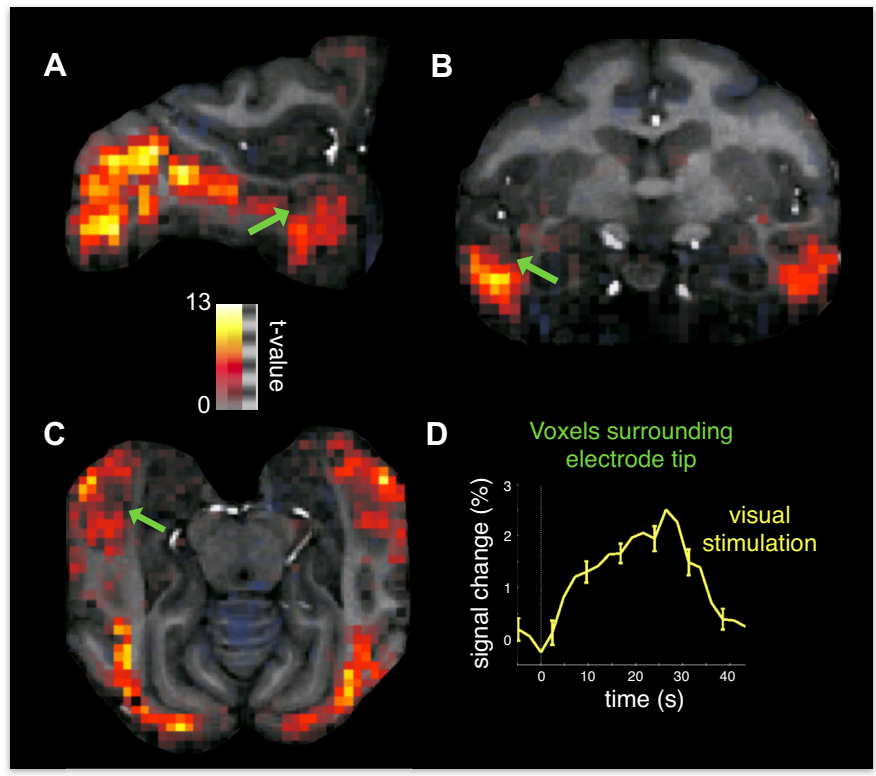

Fig. 2. Compatibility of chronic recording preparation with functional MRI. *A–C*: sagittal, coronal, and horizontal sections showing activation throughout the ventral visual pathway in a functional scan conducted postsurgically in *m1*. Each planar section includes the tip of the electrode bundle (green arrows). The electrode track is visible because of the shadow arising from magnetic susceptibility of the metal wires. *D*: time course of visually evoked activation in the cube of voxels immediately surrounding the electrode tip.

Downloaded from on November 10, 2014

implanted electrodes was not found to compromise subsequent physiological recordings in the same animals.

Longitudinal Monitoring of Single Neurons

We previously showed that the microwires employed in this study were capable of isolating spikes from single neurons from one day to the next (Bondar et al. 2009). The strategy of the present study was specifically to exploit the stability of the microwire recordings to conduct experiments that would not be feasible if recordings were limited to a single day. To this end, data were collected in seven longitudinal recording experiments (5 in *m1*, 2 in *m2*), yielding 130 neurons in total (73 from *m1*, 57 from *m2*). An overall impression of the recordings may be most readily grasped by examining a few representative examples. We focus first on three neurons in detail. Consistent with our earlier reports (Bondar et al. 2009), after an initial period of settling, spikes that appeared on a given channel on one day were often present on subsequent days. Examples of spike waveforms and ISI histograms obtained from three longitudinally monitored neurons are shown in Fig. 3. Although the spike amplitudes could sometimes vary across days, the shape of the waveforms and ISI histograms showed striking consistency over long time intervals.

Taken by itself, the day-to-day stability of waveforms recorded on each channel cannot be regarded as conclusive evidence that the spikes in fact reflect the activity of the same neurons observed on different days. But we can glean more information by assessing the consistency of visual responses, which show a high degree of stimulus selectivity in IT cortex (Richmond et al. 1987). In essence, the stimulus-specific temporal structure of each neuron's response profile can be used as a "fingerprint" for tracking the identity of individual neurons. Sample visual responses from representative neurons are shown in Fig. 4 (same 3 neurons as in Fig. 3). These neurons responded selectively to the 96 different stimuli that were presented ($P < 0.05$, ANOVA). It is clear from visual inspection of the rasters that the neurons' response patterns were largely unchanged from one day to the next. In one case (*sig073a*, Fig. 4, *bottom*), the temporal structure of visual responses was maintained despite a gap of >3 mo between the last two recordings.

To summarize the degree to which the neurons showed similar patterns of stimulus selectivity across days, we divided

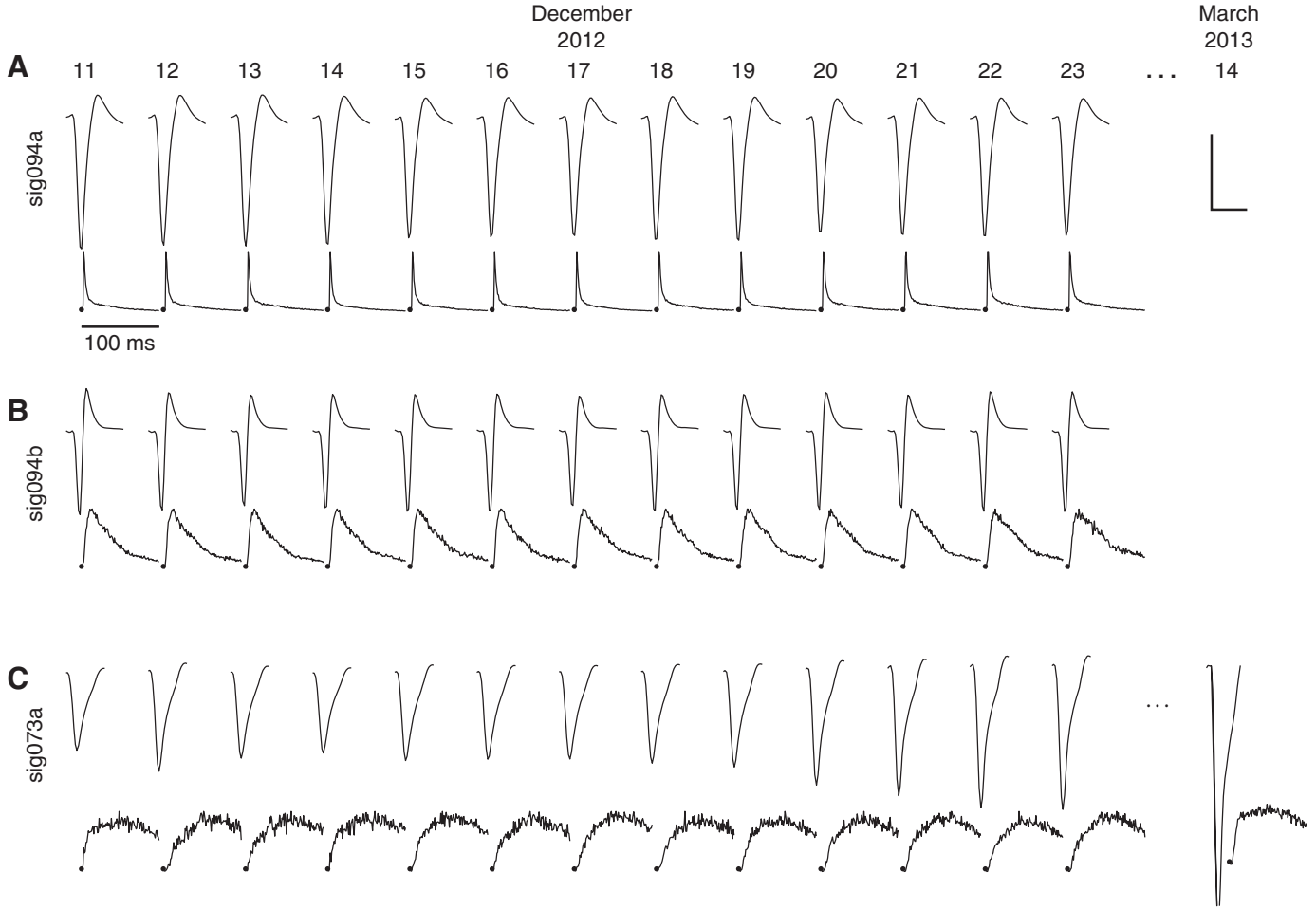

Fig. 3. Stability of longitudinally monitored spikes. *A*: mean voltage traces showing spike waveforms (*top*) and interspike interval (ISI) histograms (*bottom*) from a single neuron in *m2* that was observed in daily recording sessions over 13 days (December 11 to 23, 2012). Scale bar, 50 μV, 1 ms. *B*: spikes from a second neuron recorded simultaneously in *m2*. The spikes shown in *A* and *B* (*sig094a* and *sig094b*) were recorded on the same microwire (*channel 94*). Scale bar, 50 μV, 1 ms. *C*: spikes from a third neuron in *m2* that was observed in throughout the same 13 days in December and was still present in a follow-up recording session 3 mo later (March 14, 2013). Note the consistency in the shape of the ISI histograms across days despite the increase in spike amplitude. Scale bar, 100 μV, 1 ms.

Downloaded from on November 10, 2014

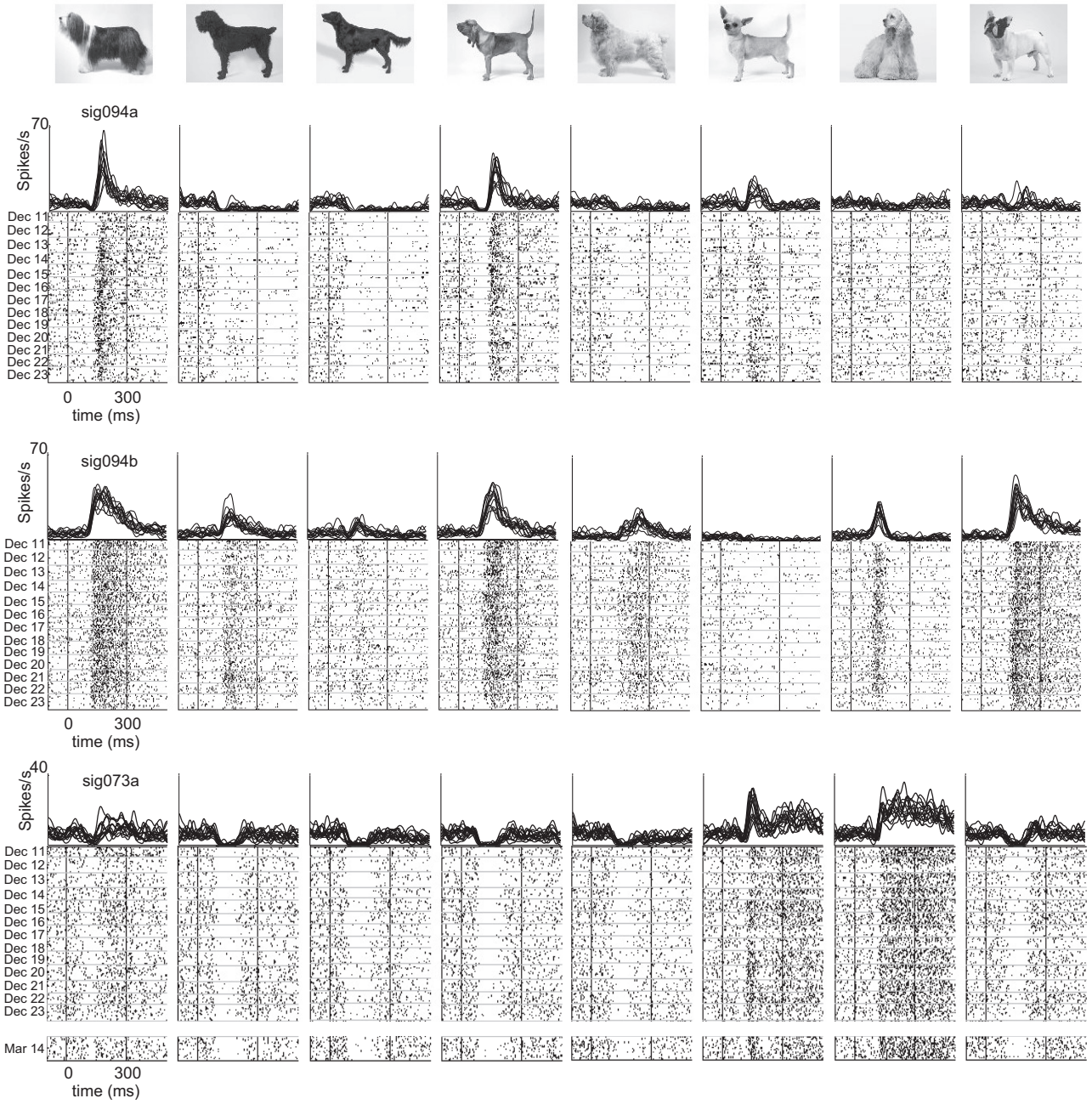

Fig. 4. Consistency of visual responses in longitudinally monitored neurons. Responses of the same 3 neurons shown in Fig. 3 to 8 images selected from a set of 96 stimuli that were presented in daily screening sessions. Daily averages of firing rate histograms (*top*) show visual responses obtained between December 11 and 23, 2012 for all neurons. A 14th session obtained on March 14, 2013 is included for 1 neuron (*sig073a*). Raster plots (*bottom*) show each trial sorted from *top* to *bottom* in chronological order. Horizontal lines in the raster plots indicate the breaks between days.

the data into split halves and computed the set of three correlation coefficients (Fig. 5*A*). We first assessed the consistency of visual responses within a single day by computing the correlation coefficient for odd and even trials taken from the same day. This within-day value ($\mathbf{r}_{within}$) provides an upper limit on how strong a correlation we can expect between two separate samples drawn from the same underlying selectivity profile. We then assessed the consistency of visual responses between two different days by computing an across-day correlation value ($\mathbf{r}_{across}$), using the odd and even trials drawn from different days. To estimate the degree of positive correlation we could expect from chance, we also computed the correlation between within-day split halves after shuffling the stimulus identities ($\mathbf{r}_{shuffle}$). We repeated this procedure for each day of recording (or, in the case of $\mathbf{r}_{across}$, between each sequential pair of days). The time course of stimulus selectivity metrics across days is shown for the three example neurons in Fig. 5*B*. The within-day and across-day correlations were nearly indistinguishable for these cells, in keeping with the subjective impression conveyed by the examples of visual responses for the same neurons shown in Fig. 4.

In addition to the 3 example neurons we have focused on thus far, 24 other neurons were recorded simultaneously over the course of one 13-day longitudinal experiment conducted in

Downloaded from on November 10, 2014

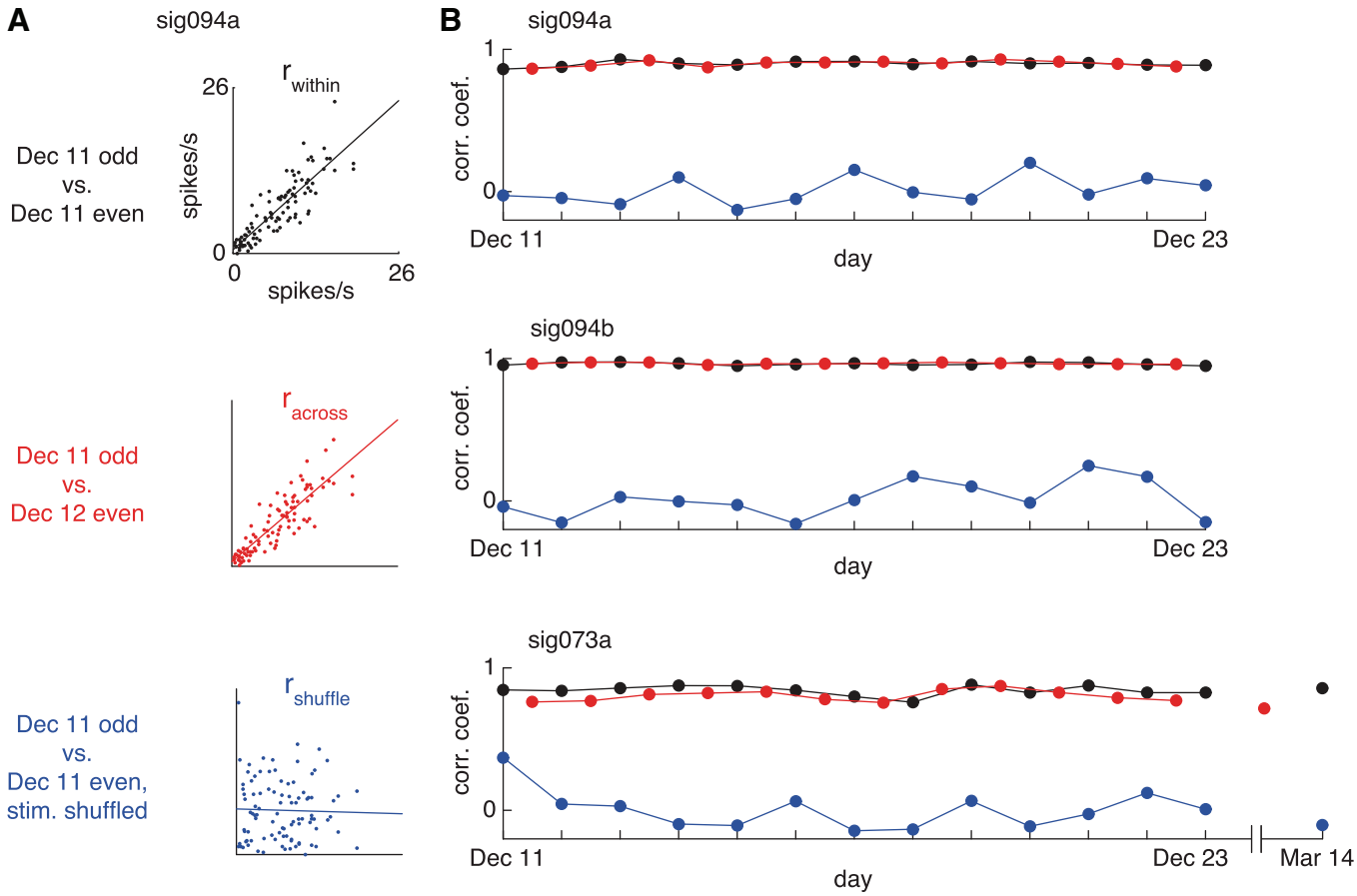

Fig. 5. Longitudinal time course of stimulus selectivity patterns. *A*: scatterplots comparing the responses of *neuron sig094a* after dividing the data into split halves of equal size. *Top*: within-day correlation ($\mathbf{r}_{within}$) computed between the mean responses to 96 stimuli on odd vs. even trials collected on the same day (December 11). *Middle*: across-day correlation ($\mathbf{r}_{across}$) computed in the same way but using split halves drawn from consecutive days (December 11 and 12). *Bottom*: stimulus-shuffled correlation ($\mathbf{r}_{shuffle}$) computed between single-day split halves after shuffling one of the halves. *B*: time course across days of stimulus selectivity metrics (computed as in *A*) for 3 neurons. Same cells as shown in Figs. 3 and 4.

December 2012. The day-to-day stability of the spike waveforms and ISI histograms for the rest of the population is summarized in Fig. 6. In total 81% of the neurons (22/27) were observed on all 13 days, and 41% (11/27) were still present in a follow-up recording session conducted 94 days later on March 14, 2013. Two fMRI scanning sessions conducted in the intervening 3 mo (on January 25 and February 8) had no obvious effect on the stability of longitudinally recorded spikes. The stimulus selectivity of these 24 neurons was again extremely consistent across days, as evidenced by the nearly overlapping within-day and across-day correlation time courses for each cell (Fig. 7*A*).

Population Summary of Longitudinal Recordings

To summarize the consistency of visual responses for the population of 130 neurons recorded in all seven longitudinal experiments, we computed a stability index for each neuron that was derived from the ratio $\mathbf{r}_{across}/\mathbf{r}_{within}$ after subtracting the stimulus-shuffled correlation value $\mathbf{r}_{shuffle}$ (see MATERIALS AND METHODS). According to this measure, a value of 1 indicates equivalent selectivity across days and between days and a value of 0 indicates no selectivity conserved across days. The distribution of stability indexes computed for the population of 130 neurons is shown in Fig. 7*B*. The fact that the distribution is clustered just to the left of 1 (median = 0.96, interquartile range 0.86–0.99) confirms the generality of the trend evident in the December 2012 data set of conserved visual responses across days. Virtually identical results were obtained by computing the stability indexes after applying a *z* transformation to the distribution of correlation coefficients. Upon finding that the visual response variability measured in this manner was small but nonzero, we assessed whether what little change there was could be attributable to changes in spike detection. Spike waveform snippets were highly correlated across days (median **r**-value 99.6, interquartile range 99.6–99.95) and not significantly correlated with changes in stimulus selectivity as computed by $\mathbf{r}_{across}$ ($P = 0.88$, *F*-test). Changes in spike amplitude between days, while typically small (median % change 3.6%, interquartile range 1.5–6.8%), were very conspicuous in some cases (as large as 55% change, as in Fig. 3*C*). However, day-to-day changes in spike amplitude were also not significantly correlated with changes in stimulus selectivity ($P = 0.88$, *F*-test). Nonetheless, we cannot rule out the possibility that changes in recording conditions across days might have contributed to measurement error in estimating visual response patterns.

The five data sets collected in *m1* were obtained sequentially after advancing the microwire bundle in bulk to a new recording site (*sets A*, *B*, and *C*) or, in two cases (*sets D* and *E*), after slightly raising the electrode bundle (Fig. 8*A*). The two data

Downloaded from on November 10, 2014

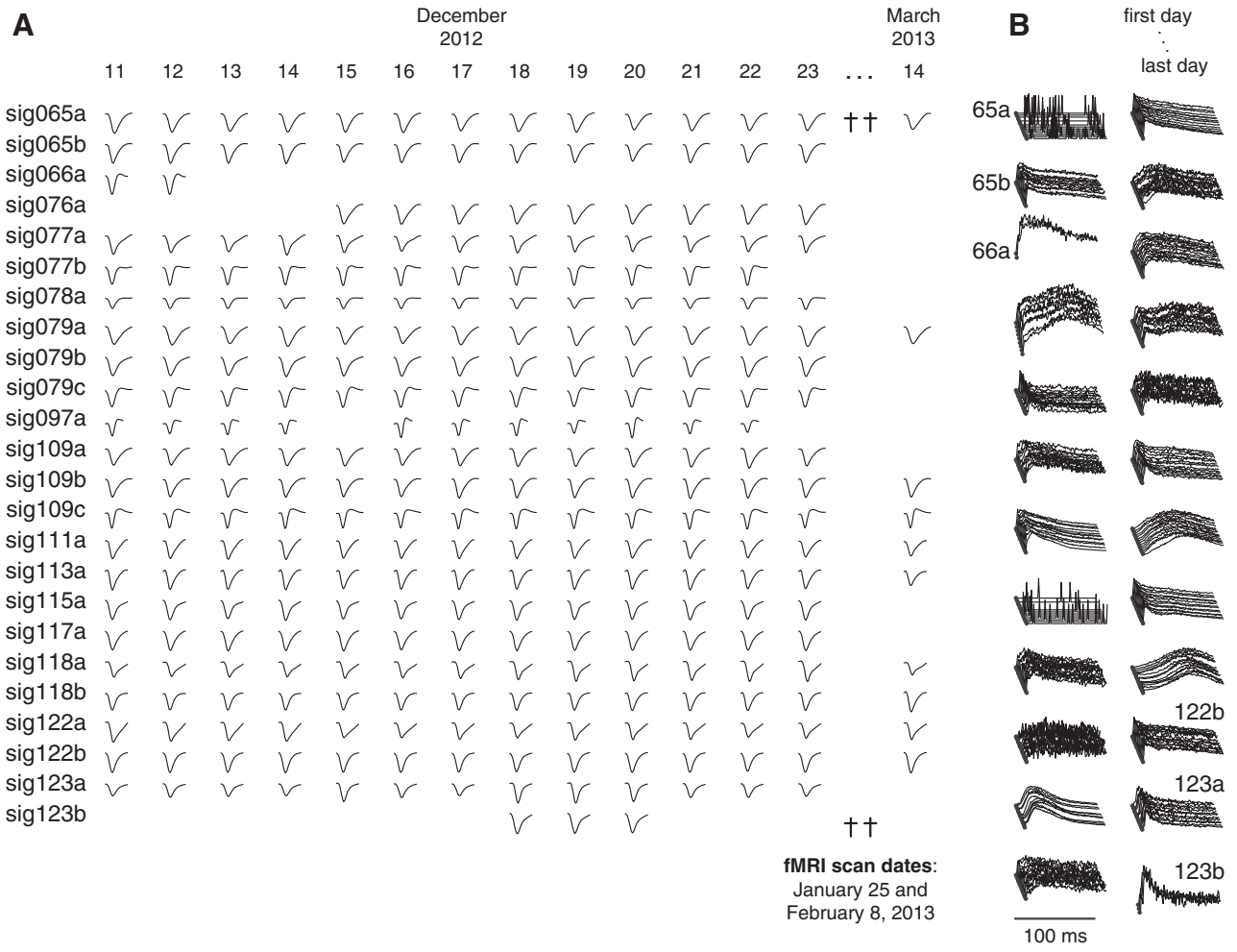

Fig. 6. Population of simultaneously recorded spikes from 1 longitudinal data set. *A*: normalized voltage traces showing the shape of the waveforms for the remainder of the neurons collected from December 11, 2012 to March 14, 2013. Functional MRI scans were conducted on 2 days in the intervening period (daggers, January 25 and February 8, 2013), which did not interfere with the ability to follow the same spikes before and after the scanning sessions. The complete population of neurons in the longitudinal session comprises the 24 neurons shown here together with the 3 neurons shown in expanded detail in Figs. 3–5. *B*: daily-averaged ISI histograms for the neurons shown in *A*.

sets from *m2* (*sets F* and *G*) were obtained 7 mo apart at the same recording depth. The neurons shown in Figs. 3–7*A* represent data *set G* in its entirety. We estimated the life span of each longitudinally monitored neuron by taking into account the preponderance of evidence drawn from the spike properties and stimulus selectivity profiles. We first considered the day-to-day stability of the spike waveforms and the shape of the ISI histograms (Bondar et al. 2009), as illustrated in Figs. 3 and 6. After excluding spikes that showed evident instability across days, we assessed the consistency of visual responses for stimulus-selective neurons using the correlation-based stability metrics (Figs. 5 and 7*A*). A visual response pattern was considered to have come from the same neuron if, for any given pair of days, the percent change across days [defined as $(\mathbf{r}_{within} - \mathbf{r}_{across})/\mathbf{r}_{within}$] was significantly greater than the percent change in the shuffled control comparison [defined as $(\mathbf{r}_{within} - \mathbf{r}_{shuffle})/\mathbf{r}_{within}$]. The stability of nonselective neurons was by necessity evaluated on the basis of spike properties. As a further reality check, the visual responses to all stimuli for all neurons were inspected manually in raster plots showing each trial on successive days (as in Fig. 4). The longevity estimates obtained according to this procedure are summarized for all 130 neurons in Fig. 8*B*. The longevity of stable recordings was at least 12 days for more than half of the neurons (mean 16.5 days, interquartile range 6–21 days). As the case of *data set G* illustrates, neurons might have continued to be present after a planned series of recordings was completed and data collection ceased. Moreover, neurons undoubtedly appeared in many cases some days prior to the commencement of daily screening sessions with the same image set. Because the longevity estimates shown in Fig. 8*B* were right- and left-censored in this way, they underestimate the true time span over which stable visual responses were actually present on the microwires.

The upper limit on how long the same neurons could be followed is hinted at by the outcome of occasional recordings in which the same stimulus set was presented in sessions spaced months apart. Figure 9 shows examples of visual responses from two neurons that were recorded simultaneously on the same microwire and showed consistent patterns of visual responses on days spanning 8 mo. Although these instances of very long-lasting neurons were exceptional cases, they indicate that the upper limit on the duration of stable

Downloaded from on November 10, 2014

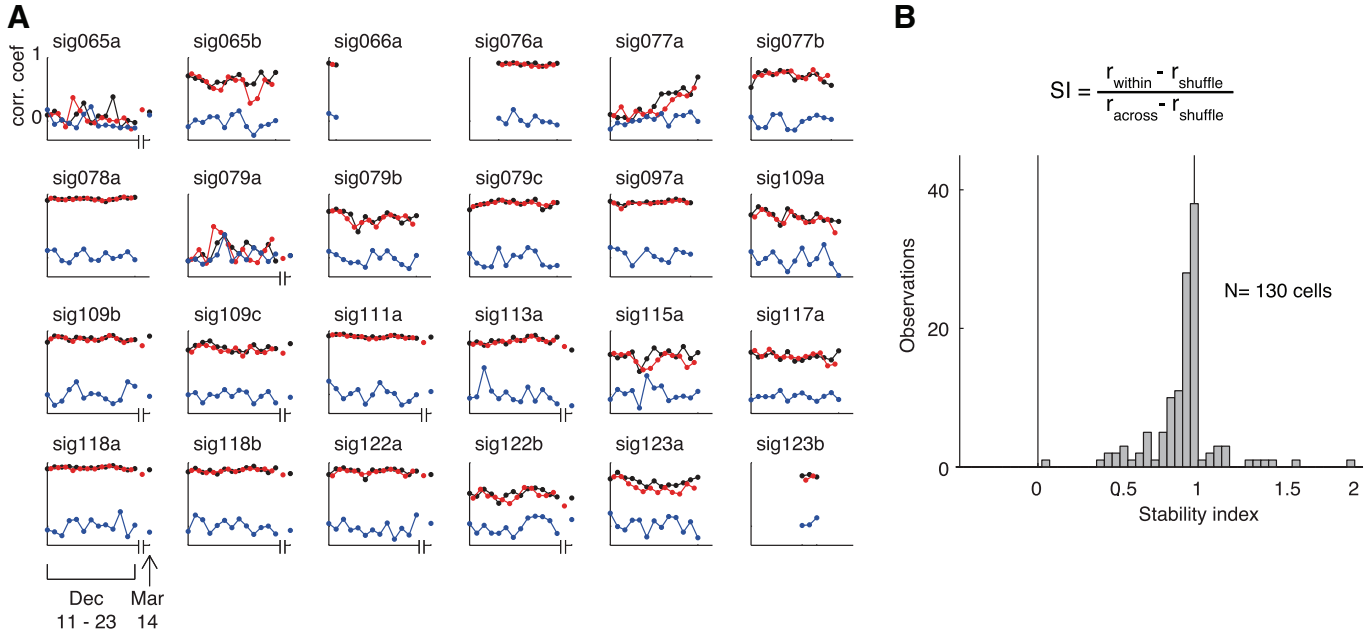

Fig. 7. Time course of stimulus selectivity patterns for 24 neurons. *A*: time course of split-halves correlation coefficients $\mathbf{r}_{within}$, $\mathbf{r}_{across}$, and $\mathbf{r}_{shuffle}$ for the 24 neurons shown in Fig. 6. Graphic conventions as in Fig. 5. *B*: distribution of stability index (SI) for 130 neurons recorded in all 7 longitudinal experiments.

recordings extends far beyond the range that we routinely sampled in the daily screening sessions.

Probing Category and Feature Selectivity with 10,000 Stimuli

When the practical constraint is removed that data collection needs to be finished within a single experimental session, it naturally follows that more trials are available for probing each neuron's responses to visual stimuli. This increase in sampling power makes it possible to assess neuronal selectivity on a much larger scale than would otherwise be feasible. We demonstrated this possibility by collecting single-unit responses to 10,000 stimuli. The complete stimulus set was too large to be viewed by the animal in a single day. Nonetheless, in record-

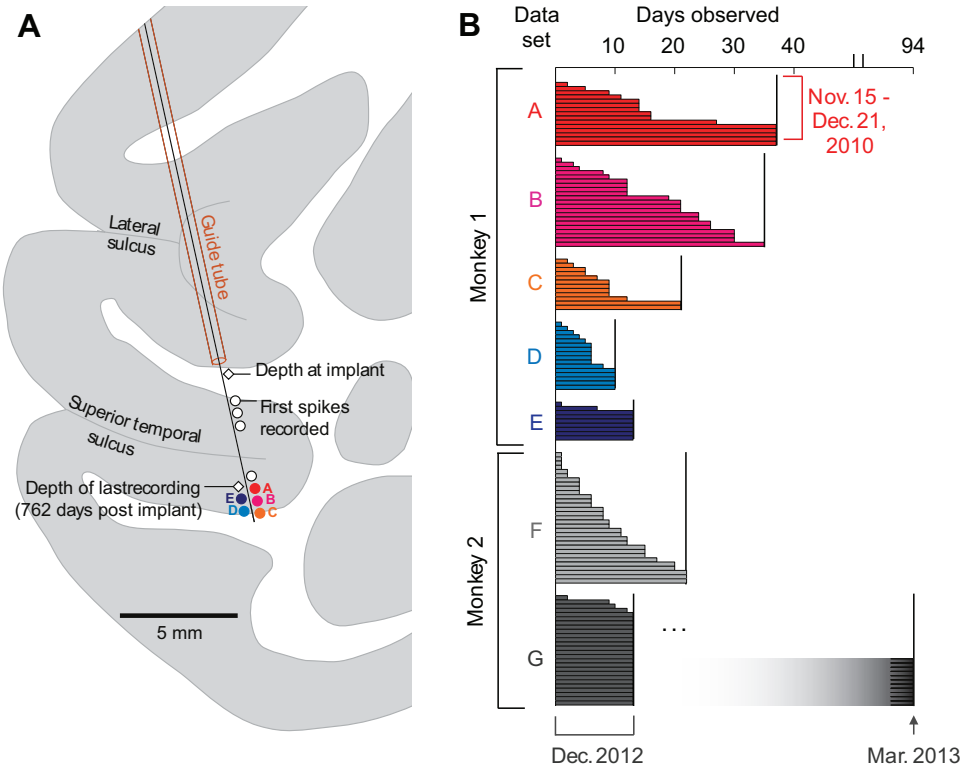

Fig. 8. Longevity of neuronal recordings obtained in 7 longitudinal experiments. *A*: diagram showing recording sites for the 5 data sets obtained in *m1* in the lower bank of the superior temporal sulcus (STS). The microwire bundle was advanced in small steps from its initial depth after surgery (white diamond) until visually responsive neurons were detected on multiple channels. Visual neurons were found in the deep layers of the lower bank (colored circles); *A–C* were encountered upon advancing the electrode and *D* and *E* upon withdrawing. White circles indicate depths where spiking activity was observed in pilot recordings prior to commencement of data collection. Spikes observed in these more dorsal sites were typically few in number and lacked obvious visual responses. *B*: longevity of 130 single-unit recordings in both monkeys. Each horizontal bar indicates the total number of days that a single neuron was observed. Colors of the 5 data sets from *m1* match the recording sites shown in *A*. The 27 neurons presented in Figs. 3–7 were recorded in *data set G*.

Downloaded from on November 10, 2014

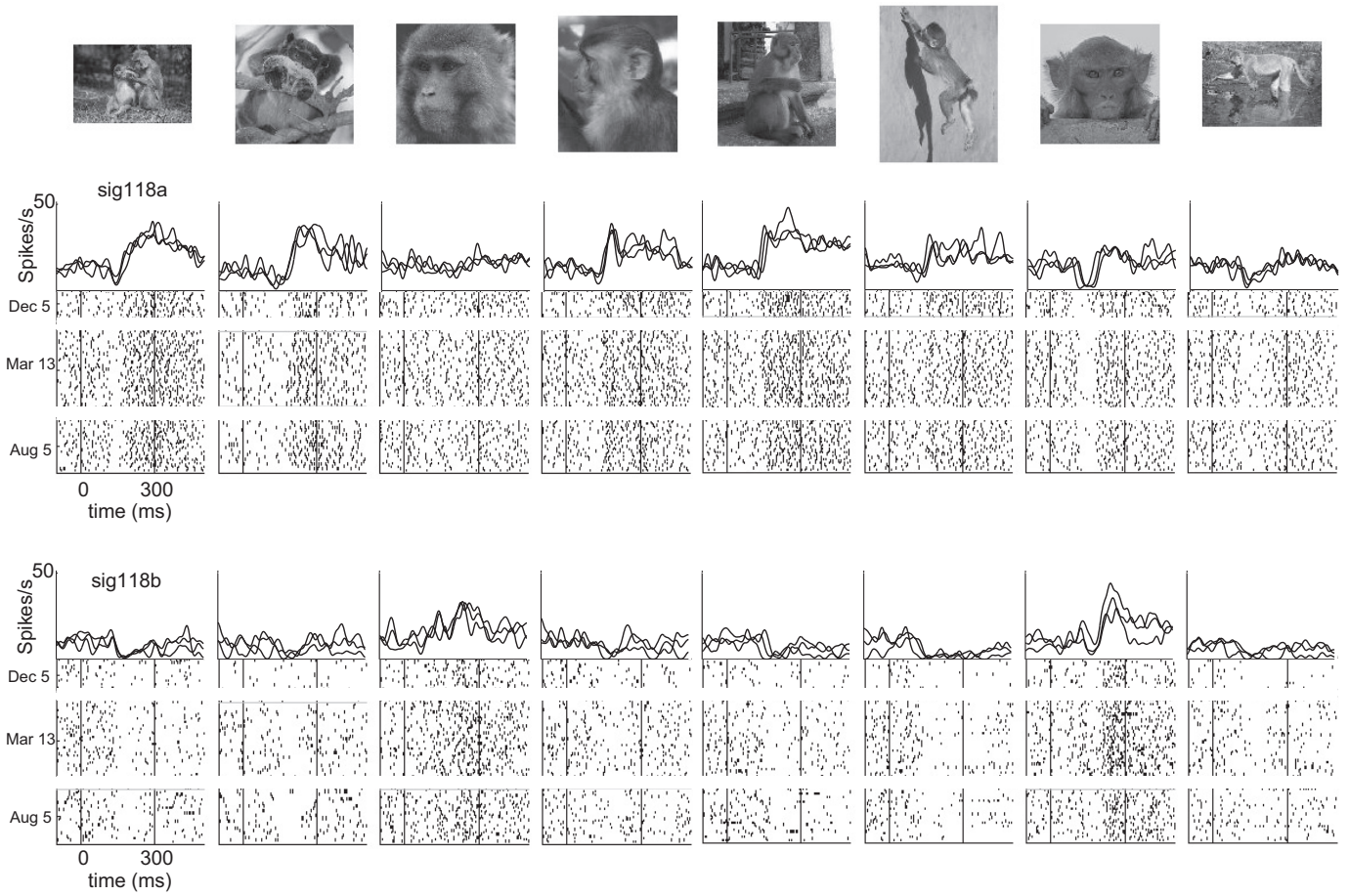

Fig. 9. Consistent patterns of visual responses observed intermittently in 2 neurons over 8 mo. Firing rate histograms show the daily-averaged visual responses of 2 neurons recorded on the same microwire in occasional experimental sessions separated by several months (December 5, 2012, March 13, 2013, and August 5, 2013). The same set of 96 stimuli was presented in each of these 3 recording sessions. Graphic conventions as in Fig. 4.

ings conducted over the course of 19 days (October 28 to November 15) several visually responsive neurons were held long enough to obtain seven or eight trials per stimulus. The complete response profile of one neuron to all stimuli is shown in Fig. 10*A*; the two rows of brightly colored pixels in the heat map indicate responses to the neuron's preferred stimulus categories, namely, human faces (*row 1*) and monkey faces (*row 3*). An expanded view of 250 images (Fig. 10*B*) revealed a strong selectivity for frontal views of human faces, as opposed to profile views, consistent with previous reports from STS neurons (Freiwald and Tsao 2010; Perrett et al. 1991). The stability of the neuron over the course of the whole experiment can be seen both in the features of the spike properties (Fig. 10*C*) and in the neuron's differential responses to individual stimuli (Fig. 10*D*). Consistent with the results of our previously presented longitudinal experiments that involved smaller stimulus sets and multiple repetitions per day, response patterns to the entire set of 10,000 stimuli were highly consistent between odd and even trials, as evident in the three neurons shown in Fig. 10*E*. The split-halves correlation was statistically significant for 30 neurons in total ($P < 0.05$, *F*-test; median correlation coefficient $r = 0.37$, interquartile range = 0.17–0.66). Thus the responses obtained were highly reliable despite the fact that they were collected on different days spanning >2 wk.

DISCUSSION

The results described here establish the feasibility of addressing new types of experimental questions with longitudinal recordings that would be beyond the reach of conventional methods. Using this approach, we found that neurons in IT cortex show a high degree of day-to-day consistency, even over timescales of many months. How does this finding compare with what we might have expected? Although longitudinal recordings from single neurons are rare in the literature, there is some reason to suspect that neurons in IT cortex undergo gradual changes on glacial timescales too slow to be detected within a single recording session. Studies of acutely sampled populations of neurons point to diminished responses to highly familiar stimuli in broadly sampled regions of IT cortex (Fahy et al. 1993; Freedman et al. 2006; Li et al. 1993; Woloszyn and Sheinberg 2012), in contrast to the stable response patterns we observed to novel and familiar images in STS (McMahon et al. 2014). Functional heterogeneity among different subregions within IT cortex may account for these differences. Early microwire recordings in area CA1 of the rodent hippocampus revealed a handful of neurons that maintained consistent place fields across many months (Thompson and Best 1990). However, more recent longitudinal studies showed that such long-lasting neurons are in the minority, and that most CA1 place cells gain or lose their spatial selectivity over the course of a

Downloaded from on November 10, 2014

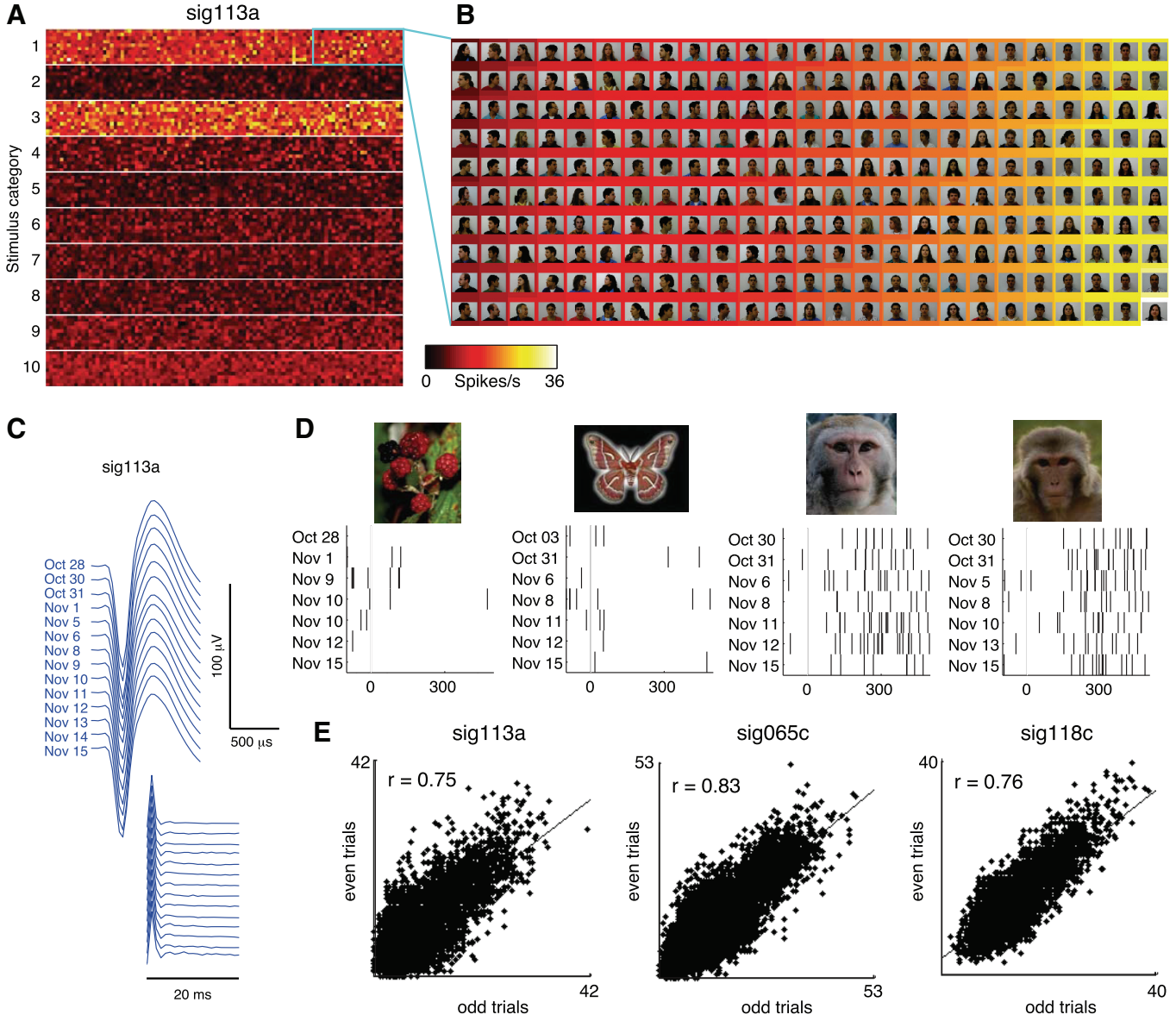

Fig. 10. Single-neuron responses to 10,000 stimuli. *A*: responses of 1 neuron to 10,000 stimuli collected over the course of 19 days, displayed in a 100 × 100 pixel matrix. The color of each pixel indicates the neuron's response to 1 stimulus, based on the mean of 7 or 8 trials collected between October 28 and November 15, 2012. The stimulus set comprised 1,000 images drawn from 10 categories: *1*) human faces, *2*) human bodies, *3*) monkey faces, *4*) monkey bodies, *5*) birds, *6*) butterflies, *7*) plants, *8*) man-made objects, *9*) scenes, and *10*) Fourier descriptors. The high firing rates evident as hot colors in the 1st and 3rd rows of the heat map indicate responses to human and monkey faces, respectively. *B*: detail of 250 human faces [representing 2.5% of the complete stimulus matrix; reproduced from the FEI face database (Thomaz and Giraldi 2010) with permission], sorted by response strength. Stimuli were sorted by the neuron's firing rate (indicated by background color) in order of weakest (*top left*) to strongest (*bottom right*). Note the neuron's stronger responses to frontal face views (hot colors on *right*) compared with profile views. *C*: spike waveform and ISI histograms from the neuron recorded in sessions between October 28 and November 15. *D*: raster plots of spikes fired by the neuron upon presentation of 4 stimuli. Consecutive trials rarely occurred on the same day (because of the large size of the stimulus set), and could occur >1 wk apart. *E*: split-halves correlations showing the consistency of stimulus selectivity for the neuron shown in *A–D* and 2 other neurons. Correlation coefficients were computed between the responses to all stimuli averaged over the odd vs. even trials from all days.

few days (Mankin et al. 2012; Ziv et al. 2013). It therefore seems likely that different brain regions will vary in their capacity to show stability or change over time.

A long-standing goal of visual neuroscience has been to elucidate the coding principles whereby objects are represented in the brain. This problem is often conceptualized in terms of discovering the organizing principles of the high-dimensional space in which objects are represented by units in a neural network (DiCarlo et al. 2012; Kourtzi and Connor 2011). Studies of feature coding most commonly proceed by specifying a limited number of hypothesized feature dimensions in advance and then testing for sensitivity to those features with tightly controlled stimulus sets (Brincat and Connor 2004; Freiwald and Tsao 2010; McMahon and Olson 2009; Nishio et al. 2012; Sripati and Olson 2010). An alternative strategy is to assess the sensitivities of single neurons or whole brain regions in a data-driven manner with larger, less constrained stimulus sets (David et al. 2006; Huth et al. 2012; Kiani et al. 2007; Kriegeskorte et al. 2008). In both of these cases, the insights gained from these experiments could be significantly enhanced

Downloaded from on November 10, 2014

by extending the range over which a given stimulus space can be explored. To the best of our knowledge, the 10,000 stimuli used here to probe neuronal selectivity represent at least an order of magnitude increase in the size of image libraries screened previously in single-unit electrophysiology. Even so, this proof-of-concept experiment employed a relatively conservative design (8 trials per stimulus, 600-ms duty cycle). It therefore seems likely that still larger stimulus spaces could be exhaustively searched by using very fast stimulus presentation rates and sparser sampling (De Baene et al. 2007; Keysers et al. 2001; Kiani et al. 2007).

The stability of recordings from implanted microwire electrodes has been noted previously and occasionally exploited (Bondar et al. 2009; Jackson and Fetz 2007; Mankin et al. 2012; Richardson et al. 2012). In most cases these studies inferred the continued presence of the same neurons from the reproducibility of waveform and spiking statistics across days. While applying these criteria is a necessary first step, some studies noted the inherent ambiguity in this approach due to the fact that similar waveforms may arise from different neurons and conversely the spikes from the same neuron may vary with slow changes in recording conditions (Dickey et al. 2009; Fraser and Schwartz 2012). The present study took the additional step of taking into account the evidence provided by the distinct temporal structure of IT visual responses (Bondar et al. 2009; Richmond et al. 1987). The stimulus specificity of this temporal structure provides a unique fingerprint for each cell and served as an additional criterion for assessing stability. Since many sensory neurons respond to time-varying stimuli with distinct and reproducible spiking patterns (Buracas et al. 1998; Mainen and Sejnowski 1995), it seems probable that the same strategy will prove effective in other brain areas as well.

There are many chronic recording methods currently in use, and the available options present a range of advantages and limitations. Floating arrays such as the Utah probe are well suited for recordings from regions on the dorsal cortical surface but are not feasible in deep brain structures. Persistence of isolated spikes across days has been reported with fixed arrays, but the usable life span of the array itself is typically limited to a window of a few months after the implant surgery (Dickey et al. 2009; Fraser and Schwartz 2012). A likely explanation for this decrease in recording yield over time is glial growth near the recording surfaces, which is commonly observed in postmortem histological sections from implanted animals. This tissue reaction presumably arises from the relative motion between the brain and rigid components of the probe (Ward et al. 2009). Semichronically fixed tungsten electrodes have occasionally been found to track neurons across days (Jackson and Fetz 2007) and further allow the possibility of advancing to a new site after the population of cells encountered at a given recording depth has been exhausted (Feingold et al. 2012). In contrast to the Utah array and other rigid electrodes, chronically implanted microwires (including both single wire bundles and braided tetrodes) commonly offer both consistent yield over time and stable monitoring of single units, as evidenced by recording studies in somatosensory and motor areas (Nicolelis et al. 1997), visual cortex (Tolias et al. 2007), hippocampus (Mankin et al. 2012), and basal ganglia (Schmitzer-Torbert and Redish 2004). The extreme fineness of the microwires used in the present study (12 μm, $\sim$10$\times$ thinner than a strand of human hair) might contribute to the longevity we and others have observed (Bondar et al. 2009; Kruger et al. 2010; Porada et al. 2000). Long-term longitudinal monitoring of single neurons is at present an emerging application, and it remains to be determined whether other recording devices could yield durable recordings comparable to the results of the present study.

The enterprise of obtaining a complete, real-time map of single-neuron activity throughout the entire brain has attracted considerable interest in recent years. The rationale for this undertaking is that, because the brain is a complex dynamical network, the principles governing its function ultimately need to be understood at the level of large-scale neuronal assemblies rather than the level of single neurons (Alivisatos et al. 2012). While this effort could be construed largely in terms of understanding the dynamics of neuronal circuits under steady-state conditions in the mature brain, we note that longitudinal monitoring of circuit dynamics over timescales relevant to development and long-term learning has the potential to yield major new insights. For practical reasons, it seems evident that the technology needed for realizing the goal of the BRAIN initiative in large-brained animals will require chronically implanted arrays of electrical, optical, and/or chemical sensors of neuronal activity. Given this necessity, the long-term stability of next-generation neuronal recording devices will be of crucial importance for realizing the potential of longitudinal monitoring of neuronal plasticity.

ACKNOWLEDGMENTS

We thank John Wittig for invaluable discussions during the early stages of designing the electrodes, Martin Bak for developing production capabilities for the electrode designs, Katy Smith and Heba Elnaiem for assistance with physiological data collection, Frank Ye, Charles Zhu, and David Yu for assistance with imaging experiments, Olga Dal Monte for assistance with stimulus library construction, and Ethan Tyler for providing the illustration in Fig. 1*B*.

GRANTS

This work was supported by National Institute of Mental Health, National Institute of Neurological Disorders and Stroke, and National Eye Institute Intramural Research Programs and by National Institutes of Health Fellowship EY-018028 to D. B. T. McMahon.

DISCLOSURES

No conflicts of interest, financial or otherwise, are declared by the author(s).

AUTHOR CONTRIBUTIONS

Author contributions: D.B.T.M., I.V.B., D.C.I., and D.A.L. conception and design of research; D.B.T.M., I.V.B., O.A.A., and D.C.I. performed experiments; D.B.T.M., O.A.A., and D.A.L. analyzed data; D.B.T.M., I.V.B., and D.A.L. interpreted results of experiments; D.B.T.M., D.C.I., and D.A.L. prepared figures; D.B.T.M. drafted manuscript; D.B.T.M. and D.A.L. edited and revised manuscript; D.B.T.M. and D.A.L. approved final version of manuscript.

REFERENCES

Alivisatos AP, Chun M, Church GM, Greenspan RJ, Roukes ML, Yuste R. The brain activity map project and the challenge of functional connectomics. *Neuron* 74: 970–974, 2012.

Baker CI, Behrmann M, Olson CR. Impact of learning on representation of parts and wholes in monkey inferotemporal cortex. *Nat Neurosci* 5: 1210–1216, 2002.

Bondar IV, Leopold DA, Richmond BJ, Victor JD, Logothetis NK. Long-term stability of visual pattern selective responses of monkey temporal lobe neurons. *PloS One* 4: e8222, 2009.

Brainard DH. The Psychophysics Toolbox. *Spat Vis* 10: 433–436, 1997.

Downloaded from on November 10, 2014

Brincat SL, Connor CE. Underlying principles of visual shape selectivity in posterior inferotemporal cortex. *Nat Neurosci* 7: 880–886, 2004.

Buracas GT, Zador AM, DeWeese MR, Albright TD. Efficient discrimination of temporal patterns by motion-sensitive neurons in primate visual cortex. *Neuron* 20: 959–969, 1998.

Churchland MM, Yu BM, Sahani M, Shenoy KV. Techniques for extracting single-trial activity patterns from large-scale neural recordings. *Curr Opin Neurobiol* 17: 609–618, 2007.

Cohen MR, Maunsell JH. Attention improves performance primarily by reducing interneuronal correlations. *Nat Neurosci* 12: 1594–1600, 2009.

Cox RW. AFNI: software for analysis and visualization of functional magnetic resonance neuroimages. *Comput Biomed Res* 29: 162–173, 1996.

David SV, Hayden BY, Gallant JL. Spectral receptive field properties explain shape selectivity in area V4. *J Neurophysiol* 96: 3492–3505, 2006.

De Baene W, Ons B, Wagemans J, Vogels R. Effects of category learning on the stimulus selectivity of macaque inferior temporal neurons. *Learn Mem* 15: 717–727, 2008.

De Baene W, Premereur E, Vogels R. Properties of shape tuning of macaque inferior temporal neurons examined using rapid serial visual presentation. *J Neurophysiol* 97: 2900–2916, 2007.

DiCarlo JJ, Zoccolan D, Rust NC. How does the brain solve visual object recognition? *Neuron* 73: 415–434, 2012.

Dickey AS, Suminski A, Amit Y, Hatsopoulos NG. Single-unit stability using chronically implanted multielectrode arrays. *J Neurophysiol* 102: 1331–1339, 2009.

Espinosa JS, Stryker MP. Development and plasticity of the primary visual cortex. *Neuron* 75: 230–249, 2012.

Fahy FL, Riches IP, Brown MW. Neuronal activity related to visual recognition memory: long-term memory and the encoding of recency and familiarity information in the primate anterior and medial inferior temporal and rhinal cortex. *Exp Brain Res* 96: 457–472, 1993.

Feingold J, Desrochers TM, Fujii N, Harlan R, Tierney PL, Shimazu H, Amemori K, Graybiel AM. A system for recording neural activity chronically and simultaneously from multiple cortical and subcortical regions in nonhuman primates. *J Neurophysiol* 107: 1979–1995, 2012.

Fraser GW, Schwartz AB. Recording from the same neurons chronically in motor cortex. *J Neurophysiol* 107: 1970–1978, 2012.

Freedman DJ, Assad JA. Experience-dependent representation of visual categories in parietal cortex. *Nature* 443: 85–88, 2006.

Freedman DJ, Riesenhuber M, Poggio T, Miller EK. Experience-dependent sharpening of visual shape selectivity in inferior temporal cortex. *Cereb Cortex* 16: 1631–1644, 2006.

Freiwald WA, Tsao DY. Functional compartmentalization and viewpoint generalization within the macaque face-processing system. *Science* 330: 845–851, 2010.

Ghose GM, Yang T, Maunsell JH. Physiological correlates of perceptual learning in monkey V1 and V2. *J Neurophysiol* 87: 1867–1888, 2002.

Gross CG, Rocha-Miranda CE, Bender DB. Visual properties of neurons in inferotemporal cortex of the Macaque. *J Neurophysiol* 35: 96–111, 1972.

Hubel DH, Wiesel TN. Early exploration of the visual cortex. *Neuron* 20: 401–412, 1998.

Hung CC, Carlson ET, Connor CE. Medial axis shape coding in macaque inferotemporal cortex. *Neuron* 74: 1099–1113, 2012.

Huth AG, Nishimoto S, Vu AT, Gallant JL. A continuous semantic space describes the representation of thousands of object and action categories across the human brain. *Neuron* 76: 1210–1224, 2012.

Jackson A, Fetz EE. Compact movable microwire array for long-term chronic unit recording in cerebral cortex of primates. *J Neurophysiol* 98: 3109–3118, 2007.

Karni A, Meyer G, Rey-Hipolito C, Jezzard P, Adams MM, Turner R, Ungerleider LG. The acquisition of skilled motor performance: fast and slow experience-driven changes in primary motor cortex. *Proc Natl Acad Sci USA* 95: 861–868, 1998.

Karni A, Sagi D. The time course of learning a visual skill. *Nature* 365: 250–252, 1993.

Keysers C, Xiao DK, Foldiak P, Perrett DI. The speed of sight. *J Cogn Neurosci* 13: 90–101, 2001.

Kiani R, Esteky H, Mirpour K, Tanaka K. Object category structure in response patterns of neuronal population in monkey inferior temporal cortex. *J Neurophysiol* 97: 4296–4309, 2007.

Kourtzi Z, Connor CE. Neural representations for object perception: structure, category, and adaptive coding. *Annu Rev Neurosci* 34: 45–67, 2011.

Kriegeskorte N, Mur M, Ruff DA, Kiani R, Bodurka J, Esteky H, Tanaka K, Bandettini PA. Matching categorical object representations in inferior temporal cortex of man and monkey. *Neuron* 60: 1126–1141, 2008.

Kruger J, Caruana F, Volta RD, Rizzolatti G. Seven years of recording from monkey cortex with a chronically implanted multiple microelectrode. *Front Neuroeng* 3: 6, 2010.

Leite FP, Tsao D, Vanduffel W, Fize D, Sasaki Y, Wald LL, Dale AM, Kwong KK, Orban GA, Rosen BR, Tootell RB, Mandeville JB. Repeated fMRI using iron oxide contrast agent in awake, behaving macaques at 3 Tesla. *Neuroimage* 16: 283–294, 2002.

Li L, Miller EK, Desimone R. The representation of stimulus familiarity in anterior inferior temporal cortex. *J Neurophysiol* 69: 1918–1929, 1993.

Mainen ZF, Sejnowski TJ. Reliability of spike timing in neocortical neurons. *Science* 268: 1503–1506, 1995.

Mankin EA, Sparks FT, Slayyeh B, Sutherland RJ, Leutgeb S, Leutgeb JK. Neuronal code for extended time in the hippocampus. *Proc Natl Acad Sci USA* 109: 19462–19467, 2012.

Matsuzaka Y, Picard N, Strick PL. Skill representation in the primary motor cortex after long-term practice. *J Neurophysiol* 97: 1819–1832, 2007.

McMahon DB, Jones AP, Bondar IV, Leopold DA. Face-selective neurons maintain consistent visual responses across months. *Proc Natl Acad Sci USA* 111: 8251–8256, 2014.

McMahon DB, Olson CR. Linearly additive shape and color signals in monkey inferotemporal cortex. *J Neurophysiol* 101: 1867–1875, 2009.

Merzenich MM, Nelson RJ, Stryker MP, Cynader MS, Schoppmann A, Zook JM. Somatosensory cortical map changes following digit amputation in adult monkeys. *J Comp Neurol* 224: 591–605, 1984.

Nicolelis MA, Dimitrov D, Carmena JM, Crist R, Lehew G, Kralik JD, Wise SP. Chronic, multisite, multielectrode recordings in macaque monkeys. *Proc Natl Acad Sci USA* 100: 11041–11046, 2003.

Nicolelis MA, Ghazanfar AA, Faggin BM, Votaw S, Oliveira LM. Reconstructing the engram: simultaneous, multisite, many single neuron recordings. *Neuron* 18: 529–537, 1997.

Nishio A, Goda N, Komatsu H. Neural selectivity and representation of gloss in the monkey inferior temporal cortex. *J Neurosci* 32: 10780–10793, 2012.

Perrett DI, Oram MW, Harries MH, Bevan R, Hietanen JK, Benson PJ, Thomas S. Viewer-centred and object-centred coding of heads in the macaque temporal cortex. *Exp Brain Res* 86: 159–173, 1991.

Porada I, Bondar I, Spatz WB, Kruger J. Rabbit and monkey visual cortex: more than a year of recording with up to 64 microelectrodes. *J Neurosci Methods* 95: 13–28, 2000.

Recanzone GH, Merzenich MM, Jenkins WM, Grajski KA, Dinse HR. Topographic reorganization of the hand representation in cortical area 3b owl monkeys trained in a frequency-discrimination task. *J Neurophysiol* 67: 1031–1056, 1992.

Richardson AG, Borghi T, Bizzi E. Activity of the same motor cortex neurons during repeated experience with perturbed movement dynamics. *J Neurophysiol* 107: 3144–3154, 2012.

Richmond BJ, Optican LM, Podell M, Spitzer H. Temporal encoding of two-dimensional patterns by single units in primate inferior temporal cortex. I. Response characteristics. *J Neurophysiol* 57: 132–146, 1987.

Sanes JN, Donoghue JP. Plasticity and primary motor cortex. *Annu Rev Neurosci* 23: 393–415, 2000.

Schmitzer-Torbert N, Redish AD. Neuronal activity in the rodent dorsal striatum in sequential navigation: separation of spatial and reward responses on the multiple T task. *J Neurophysiol* 91: 2259–2272, 2004.

Schoups A, Vogels R, Qian N, Orban G. Practising orientation identification improves orientation coding in V1 neurons. *Nature* 412: 549–553, 2001.

Scott SH. Inconvenient truths about neural processing in primary motor cortex. *J Physiol* 586: 1217–1224, 2008.

Sergio LE, Hamel-Paquet C, Kalaska JF. Motor cortex neural correlates of output kinematics and kinetics during isometric-force and arm-reaching tasks. *J Neurophysiol* 94: 2353–2378, 2005.

Sigala N, Logothetis NK. Visual categorization shapes feature selectivity in the primate temporal cortex. *Nature* 415: 318–320, 2002.

Sripati AP, Olson CR. Responses to compound objects in monkey inferotemporal cortex: the whole is equal to the sum of the discrete parts. *J Neurosci* 30: 7948–7960, 2010.

Thomaz CE, Giraldi GA. A new ranking method for principal components analysis and its application to face image analysis. *Image Vision Comput* 28: 902–913, 2010.

Thompson LT, Best PJ. Long-term stability of the place-field activity of single units recorded from the dorsal hippocampus of freely behaving rats. *Brain Res* 509: 299–308, 1990.

Downloaded from on November 10, 2014

Tolias AS, Ecker AS, Siapas AG, Hoenselaar A, Keliris GA, Logothetis NK. Recording chronically from the same neurons in awake, behaving primates. *J Neurophysiol* 98: 3780–3790, 2007.

Ward MP, Rajdev P, Ellison C, Irazoqui PP. Toward a comparison of microelectrodes for acute and chronic recordings. *Brain Res* 1282: 183–200, 2009.

Woloszyn L, Sheinberg DL. Effects of long-term visual experience on responses of distinct classes of single units in inferior temporal cortex. *Neuron* 74: 193–205, 2012.

Xiang QS, Ye FQ. Correction for geometric distortion and N/2 ghosting in EPI by phase labeling for additional coordinate encoding (PLACE). *Magn Reson Med* 57: 731–741, 2007.

Yamane Y, Carlson ET, Bowman KC, Wang Z, Connor CE. A neural code for three-dimensional object shape in macaque inferotemporal cortex. *Nat Neurosci* 11: 1352–1360, 2008.

Ziv Y, Burns LD, Cocker ED, Hamel EO, Ghosh KK, Kitch LJ, El Gamal A, Schnitzer MJ. Long-term dynamics of CA1 hippocampal place codes. *Nat Neurosci* 16: 264–266, 2013.

Downloaded from on November 10, 2014